

Non-Inductive Current Drive Modeling Extending Advanced Tokamak Operation to Steady State

*T.A. Casper, L.L. Lodestro, L.D. Pearlstein, G.D. Porter,
M. Murakami, L.L. Lao, Y.R. Lin-Liu, H.E. St. John*

This article was submitted to
27th European Physical Society Conference on Controlled Fusion
and Plasma Physics, Budapest, Hungary, June 12-16, 2000

U.S. Department of Energy

Lawrence
Livermore
National
Laboratory

June 6, 2000

DISCLAIMER

This document was prepared as an account of work sponsored by an agency of the United States Government. Neither the United States Government nor the University of California nor any of their employees, makes any warranty, express or implied, or assumes any legal liability or responsibility for the accuracy, completeness, or usefulness of any information, apparatus, product, or process disclosed, or represents that its use would not infringe privately owned rights. Reference herein to any specific commercial product, process, or service by trade name, trademark, manufacturer, or otherwise, does not necessarily constitute or imply its endorsement, recommendation, or favoring by the United States Government or the University of California. The views and opinions of authors expressed herein do not necessarily state or reflect those of the United States Government or the University of California, and shall not be used for advertising or product endorsement purposes.

This is a preprint of a paper intended for publication in a journal or proceedings. Since changes may be made before publication, this preprint is made available with the understanding that it will not be cited or reproduced without the permission of the author.

This report has been reproduced
directly from the best available copy.

Available to DOE and DOE contractors from the
Office of Scientific and Technical Information
P.O. Box 62, Oak Ridge, TN 37831
Prices available from (423) 576-8401
<http://apollo.osti.gov/bridge/>

Available to the public from the
National Technical Information Service
U.S. Department of Commerce
5285 Port Royal Rd.,
Springfield, VA 22161
<http://www.ntis.gov/>

OR

Lawrence Livermore National Laboratory
Technical Information Department's Digital Library
<http://www.llnl.gov/tid/Library.html>

Non-Inductive Current Drive Modeling Extending Advanced Tokamak Operation to Steady State

T.A. Casper¹, L.L. LoDestro¹, L.D. Pearlstein¹, G.D. Porter¹, M. Murakami²,
L.L. Lao³, Y.R. Lin-Liu³, and H.E. St.John³

¹Lawrence Livermore National Laboratory, Livermore, California, USA

²Oak Ridge National Laboratory, Oak Ridge, Tennessee, USA

³General Atomics, San Diego, California, USA

A critical issue for sustaining high performance, negative central shear (NCS) discharges is the ability to maintain current distributions that are maximum off axis. Sustaining such hollow current profiles in steady state requires the use of non-inductively driven current sources. On the DIII-D experiment, a combination of neutral beam current drive (NBCD) and bootstrap current have been used to create transient NCS discharges. The electron cyclotron heating (ECH) and current drive (ECCD) system is currently being upgraded from three gyrotrons to six to provide more than 3MW of absorbed power in long-pulse operation to help sustain the required off-axis current drive. This upgrade supports the long range goal of DIII-D to sustain high performance discharges with high values of normalized β , $\beta_N = \beta / (I_p / a B_T)$, confinement enhancement factor, H, and neutron production rates while utilizing bootstrap current fraction, f_{bs} , in excess of 50%. At these high performance levels, the likelihood of onset of MHD modes that spoil confinement indicates the need to control plasma profiles if we are to extend this operation to long pulse or steady state.

To investigate the effectiveness of the EC system* and to explore operating scenarios to sustain these discharges, we use time-dependent simulations of the equilibrium, transport and stability. We explore methods to directly alter the safety factor profile, q, through direct current drive or by localized electron heating to modify the bootstrap current profile. Time dependent simulations using both experimentally determined [1] and theory-based [2] energy transport models have been done. Here, we report on simulations exploring parametric dependencies of the heating, current drive, and profiles that affect our ability to sustain stable discharges.

In these simulations, we primarily use the Corsica equilibrium and transport code [3] which self-consistently solves for both equilibrium and transport at each step in the temporal evolution. The equilibrium is provided by a kinetic solution to the inverse Grad-Shafranov equation using the pressure profile obtained from a combination of measured and transported fields. Thermal density profiles are provided either by the experimental density measurements or an analytic model profile and the fast ion density provided by a Monte Carlo simulation of neutral beam injection. The impurity fraction is provided by the measured effective charge state, Z_{eff} , assuming fully ionized carbon impurities. Entropy profiles are evolved using a heat conductivity model based on a gyro-Bohm scaling [2]. We use $\chi_e = c_e (T_e^{3/2} / B^2) (T_e / T_i)^{\alpha} f(s) q^2 + \chi_e^{neo} + \chi_{edge}$ for the heat conductivity where $f(s) = 1 / [1 + (9/4)(s - 2/3)^2]$, $s = (\rho / q) \partial q / \partial \rho$ is the shear parameter ($\rho =$ toroidal flux), $c_e = 1.4$ is chosen to approximate the initial experimentally measured temperature profile, $\alpha = 1$ for the temperature ratio dependence, χ_e^{neo} is the electron neoclassical heat conductivity and χ_{edge} is used to control the edge heat conductivity consistent with edge modeling and convergence requirements. This representation provides a weak electron thermal transport barrier. The ion thermal conductivity is modeled as, $\chi_i = c_i \chi_e H(\nabla q) Z_{eff} (T_e / T_i)^{1/2} + \chi_i^{neo}$ where $c_i = 1.0$, χ_i^{neo} is the ion neoclassical heat conductivity and $H(\nabla q)$ is the Heaviside function which turns on at the q_{min}

*Work supported by U.S. Dept. of Energy under Contracts W-7405-ENG-48 (LLNL) and DE-AC03-89ER51114 (GA)

location. This gives a strong ion thermal transport barrier at the location of the minimum of q , ρ_{qmin} . The Heaviside function provides independent control over the diffusivity inside the barrier so as to match the initial measured ion temperature profile.

We initialized simulations at an arbitrary time using experimentally measured density, temperature and Z_{eff} profiles and a boundary shape determined from EFIT [4] using both magnetic and motional Stark effect measurements to constrain the fitting process. By converging a free boundary equilibrium solution in Corsica to the EFIT solution we achieve good agreement between the plasma shape and q -profile. We use a fixed boundary calculation and resistive current diffusion to evolve the current density and q profiles. An assessment of the time-dependent MHD stability of the resulting equilibria is provided by the DCON [5] stability code that we have added to the Corsica suite. We use Gaussian approximations to the ECH power deposition and current drive profiles with the shape adjusted based on comparisons with TORAY ray tracing calculations with the ONETWO code [1]. ECCD current drive is given by $I_{ECCD} = \gamma P_{ECH} T_e / n_e R$ where the efficiency, γ , is determined from experimental measurements [1]. The neutral-beam-driven current is given by the Monte Carlo deposition model with orbit calculations used to determine the current drive contributions from the particle residence time in each flux surface and the assumption of a dragged-down distribution.

We performed several simulations for the DIII-D shot number 92668 that is representative of several high performance negative central shear discharges obtained with L-mode edge profiles. Parameters at initialization for this shot are 1.4MA plasma current, 10MW neutral beam injection, peak electron density of $0.7 \times 10^{20} m^{-3}$, on-axis temperatures of 6keV for electrons and 19keV ions. Simulations are initialized at 1.45s into the discharge, just prior to a β -collapse resulting from MHD activity due to the internally peaked pressure profile obtained with neutral beam fueling. The EC heating power and location were varied to investigate the duration that the NCS configuration

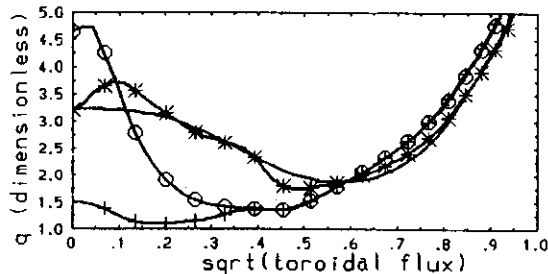
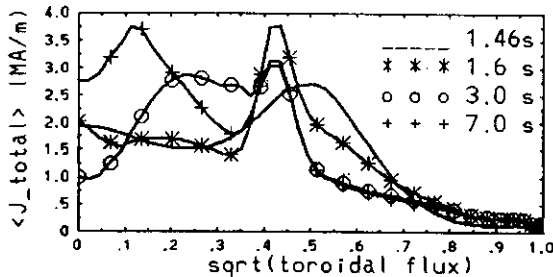


Fig.1 Flux-averaged total current density and q profiles at initialization (1.46s), $2\tau_E$ after ECH applied (1.6s), just prior to barrier loss (3.0s) and late time (7.0s).

can be maintained. Through a combination of direct ECCD and electron heating to increase the temperature gradient and thus the bootstrap current, the NCS configuration can be maintained for long duration when sufficient power is absorbed. The local peaking of the current density profile (and therefore a depression in q) sustains the barrier and maintains the location of ρ_{qmin} [2].

At 1.5 seconds we turned on ECH in these simulations and force the boundary loop voltage to zero in order to find non-inductively-driven steady-state configurations. EC absorbed power levels of 0, 1, 2.3 (3MW injected), 4.5 (6MW injected), 7.5 and 9 MW were used with $P_{NB}=10$ MW held fixed. The 3MW injected case corresponds to power levels soon available on DIII-D with 6MW a future upgrade. In Fig. 1, we show the radial profiles of the total flux-averaged current density, $\langle J_T \rangle = \langle J \cdot B \rangle / \langle B \cdot \nabla \psi \rangle$, and the q profiles achieved for the 4.5MW case with power applied at $\rho=0.425$, just inside the ρ_{qmin} formed with early neutral beam injection during the current ramp. When ECH is initially applied (at 1.6s), it

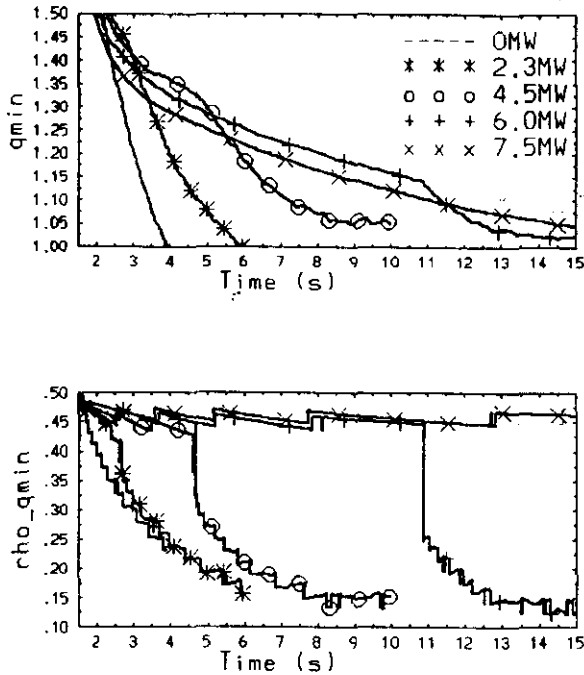


Fig. 2 q_{min} and ρ_{qmin} versus time as a function of ECH absorbed power indicating power dependence for sustaining NCS

at lower power levels than when heating at $\rho=0.5$. Ultimately, the NCS configuration is lost due to on-axis peaking of the current density or the q profile dropping below 1 at some radius (at which time the simulations are stopped).

To explore the effects of density control on performance, we ran simulations with the density profile scaled to 90% and 80% of the measured values for the heating location at $\rho=0.425$. The increased power per particle available provides a further enhancement of the efficacy of ECH for sustaining such NCS discharges. As observed in Fig. 3 for 4.5MW, we obtain a factor of 5 increase in duration that the NCS configuration can be sustained at 80% density. To further explore the advantages of density profile control, we used a model density profile (rather than the scaled measured profile) of the form $n(\rho) \propto n_0 / (1 + a_\rho (\rho/\rho_0)^2)$ adjusted to fix the peak density at the measured value of $.7 \times 10^{20}$ and to place the density gradient near the heating location. This optimizes the location of the density gradient driven bootstrap current profile and provides better alignment of the overall total current profile. In Fig. 3, we observe a further increase in the duration that the NCS configuration can be maintained. Exploring this advantage of density control is one motivation for our beginning to do simulations with our core transport code coupled to the UEDGE [6] code.

results in a local perturbation of the q profile along with inductively induced changes near the magnetic axis. At this power level and heating location, the NCS configuration is maintained for $\sim 3.5s$ at which time the Ohmic current has diffused inward and resistively decayed, particularly in the more resistive outer region, and the barrier begins to move inward. At late times when the OH current is low, the total internal current distribution is dominated by the neutral beam current drive that is peaked on axis for the injection geometry on DIII-D and the bootstrap current. As a figure of merit of barrier maintenance, we take the time duration that ρ_{qmin} is held fixed just outside the EC deposition location. Due to current diffusion and dissipation, at low to moderate EC power levels the position of q_{min} eventually moves in at the resistive current diffusion rate [2] as indicated in Fig. 2. We summarize in Fig. 3 a series of simulations where the power and heating location are varied. We observe that when power is absorbed at the $\rho=0.425$ location, the better alignment of the ECCD with the bootstrap current allows us to sustain the desired current profiles for much longer duration

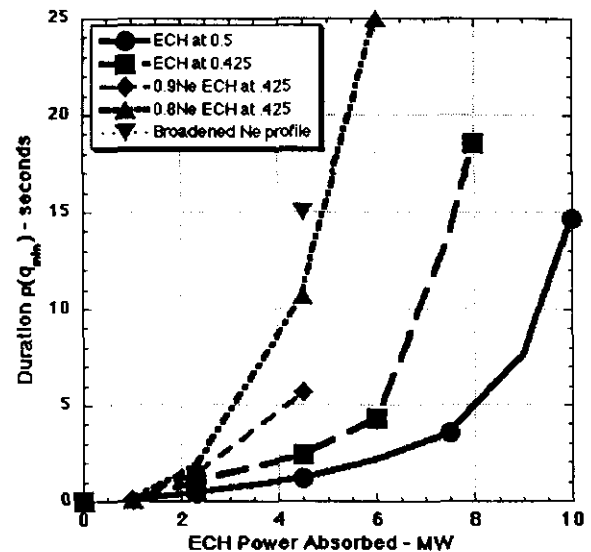


Fig. 3 Duration that ρ_{qmin} is held fixed as a function of ECH power applied at $\rho=0.5$ (barrier) and 0.425 (inside barrier) with density dependence.

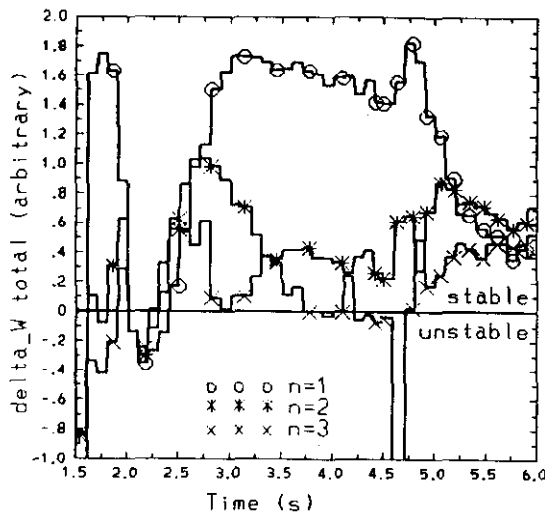


Fig. 4 Evolution of δW for 4.5MW heating case from DCON ideal stability analysis for toroidal mode numbers $n=1, 2$ and 3 . $\delta W < 0$ for instability.

We use the DCON [5] code to assess MHD stability during simulated discharge evolution. DCON calculates the minimum potential energy δW to assess overall stability to ideal MHD, internal and ballooning modes. In Fig. 4, we show δW_{total} ($=\delta W_{\text{plasma}}+\delta W_{\text{vacuum}}>0$ for stability) for toroidal mode numbers $n=1, 2$ and 3 for the 4.5MW case. We note that shortly after initialization ($t=1.5\text{s}$) and without heating, DCON predicts instability for all three mode numbers and, indeed, the discharge disrupted at 1.57s. During the formation phase of the self-consistent driven current profile shortly after ECH is applied ($1.5<t<2.3\text{s}$), we observe that instability is predicted at the various mode numbers analyzed at various times. This is likely due to the highly peaked current density at the ECH location (e.g. see 1.6s shown in Fig. 1. where $q\sim 2$). One effect of the ECH heating is to broaden the electron temperature profile to the heating location at $p=0.425$. Similarly, the effects of

heating and the transport model is to provide relatively flat temperature profiles inside the minimum of q . These broadened profiles along with modifications in the parallel current distribution due to ECCD have resulted in stabilization of these MHD modes for this simulation as observed from $\delta W_{\text{total}} > 0$ after 2.3s. We observe a destabilization of the $n=3$ mode at the time the barrier was lost (4.7s) at both 3 and 6MW but this detail has not been studied.

Time dependent simulations of the effect of electron cyclotron heating and current drive indicate that at sufficiently high absorbed powers, L-mode edge NCS discharges can be sustained for very long pulse duration. The configuration exhibits a fully non-inductively driven state formed from a combination of bootstrap, neutral beam and electron cyclotron current drive. Ideal MHD stability calculations indicate these profiles evolve in a stable configuration over the full duration. For this case, primarily due to the high power density under the L-mode edge conditions, ECCD plays a dominant role in controlling the q profile. Late time, on-axis current distribution is, however, dominated by the NBCD which could be improved by changes in the neutral beam injection geometry or by shifting the plasma to move the current drive off axis. At the EC power levels soon to be available on DIII-D, significant effects will be observable during experiments. With upgrades to the ECH system, near non-inductively driven configurations may be obtained on the time scales of the magnetic field pulse available on DIII-D. Density control, particularly the ability to contour the density gradient location, could provide distinct advantages for optimizing the discharge and achieving steady state configurations.

[1] Masanori, M., et al., IAEA TCM on Steady State Operations, Nuclear Fusion, June 2000 Vol. 40 (6) 1025-1286.

[2] Casper, T. A., et al., Proc. 25th EPS Conference On Controlled Fusion and Plasma Physics, Prague, Czech Republic, p3.190 (p652) June 29-July 3, 1998.

[3] Crotinger, J. A., et al., LLNL Report, UCRL-ID-126284, March 19, 1997.

[4] Lau, L., <http://lithos.gat.com/efit>.

[5] Glasser, A.H., LANL Report, LA-UR-95-528, February 1995.

[6] Rognlien, T.D., et al., Contr. Plasma Phys., 1994. 34(2/3) p. 362-367.